

# **Analysis of hemodynamics and angiogenic response to ischemia in the obese type 2 diabetic model Spontaneously Diabetic Torii *Lepr<sup>fa</sup>* (SDT fatty) rats**

**Yasutaka Murai<sup>1,2</sup>, Tomohiko Sasase<sup>1</sup>, Hironobu Tadaki<sup>1</sup>, Shiro Heitaku<sup>1</sup>, Naoya Imagawa<sup>1</sup>, Takahisa Yamada<sup>2,3</sup>, Takeshi Ohta<sup>3</sup>**

<sup>1</sup>Japan Tobacco Inc., Central Pharmaceutical Research Institute, 1-1, Murasaki-cho, Takatsuki, Osaka 569-1125, Japan

<sup>2</sup>Faculty of Agriculture, Department of Agrobiolgy, Niigata University, Nishi-ku, Niigata 950-2181, Japan

<sup>3</sup>Laboratory of Animal Physiology and Functional Anatomy, Graduate School of Agriculture, Kyoto University, Kitashirakawa, Sakyo-ku, Kyoto 606-8502, Japan

## **Short title**

Hemodynamics in a new type 2 diabetic rat model

## **Corresponding author**

Y. Murai, Japan Tobacco Inc., Central Pharmaceutical Research Institute, 1-1, Murasaki-cho, Takatsuki, Osaka 569-1125, Japan. E-mail: [yasutaka.murai@jt.com](mailto:yasutaka.murai@jt.com)

## Abstract

Peripheral artery disease (PAD) is defined as peripheral blood flow impairment, especially in the legs, caused by atherosclerotic stenosis. The disease decreases quality of life because of intermittent claudication or necrosis of the leg. The hindlimb ischemia model, in which ischemia is induced by femoral artery ligation, is often utilized as a PAD model. In the hindlimb ischemia model, nonmetabolic syndrome animals are mainly used. In this study, we investigated the usefulness of Spontaneously Diabetic Torii *Lep<sup>fa</sup>* (SDT fatty) rats, a new model for obese type 2 diabetes, as a new PAD animal model. We found that hindlimb blood flow in SDT fatty rats was significantly lower than that in Sprague–Dawley (SD) rats under nonischemic conditions. Furthermore, SDT fatty rats showed a significantly higher plasma nitrogen oxide level, shorter prothrombin time, and shorter activated partial thromboplastin time than SD rats. In addition, we found that the change in blood flow 7 days after induction of hindlimb ischemia and the number of Von Willebrand Factor-positive vessels in gastrocnemius muscles were significantly lower in SDT fatty rats than in SD rats. These results suggest that excess production of reactive oxygen species and coagulation activation could be involved in lower blood flow in nonischemic rats and that decreased angiogenesis could be involved in the poor recovery of blood flow in SDT fatty rats with hindlimb ischemia. Taken together, our results suggest that SDT fatty rats might be useful as a new model for PAD with metabolic syndrome.

**Keywords**

angiogenesis, coagulation, endothelial function, hemodynamics, hindlimb blood flow, ischemia, peripheral artery disease, SDT fatty rats

## **Introduction**

Peripheral artery disease (PAD) is defined as peripheral blood flow impairment, especially in the legs, caused by atherosclerotic stenosis. The risk factors for PAD are age, smoking, hypertension, diabetes, and dyslipidemia.<sup>1</sup> Although initially asymptomatic, PAD induces intermittent claudication and finally leg necrosis. Therefore, PAD limits the activity of daily living and decreases the quality of life (QOL). Furthermore, PAD patients have a high risk of cardiovascular events because most of these patients have atherosclerotic stenosis not only in the arteries of the legs but also in the cardiovascular system.<sup>2</sup> The worldwide prevalence of PAD is about 3% to 10% and increases to 15% to 20% in people over 70 years old.<sup>1</sup>

The goals of PAD treatment are prevention of cardiovascular events and improvement of leg symptoms, including intermittent claudication and necrosis. The main treatments for preventing cardiovascular events are risk factor modifications, including controlling the level of low-density lipoprotein (LDL) cholesterol, blood glucose, blood pressure, and antiplatelet therapy, and smoking cessation. The three main treatments for improving leg symptoms are supervised exercise, cilostazol, and revascularization.<sup>3,4</sup> However, new treatments for leg symptoms are needed because these three treatments are limited by physical and economic burdens, side effects, and restenosis.

The hindlimb ischemia model, in which ischemia is induced by femoral artery ligation, is often utilized as a PAD model in nonclinical studies. In the hindlimb ischemia model,

nonmetabolic syndrome animals, such as C57BL/6J and BALB/c mice, are mainly used. However, many PAD patients have some components of metabolic syndrome such as hypertension, diabetes, and dyslipidemia in their background<sup>1</sup> and show endothelial dysfunction.<sup>5</sup> Therefore, it is very important to establish a PAD model based on metabolic syndrome in animals. Some groups have attributed the poor recovery of hindlimb blood flow after hindlimb ischemia in type 2 diabetic *db/db* mice or streptozotocin (STZ)-induced type 1 diabetic mice to the impairment of the angiogenic response to ischemia in diabetic animals.<sup>6,7</sup>

Spontaneously Diabetic Torii *Lep<sup>fa</sup>* (SDT fatty) rats were established by transferring the *fa* allele of the Zucker fatty rat into the genome of the nonobese SDT rat. The SDT fatty rat shows hyperphagia, obesity, hyperglycemia, and dyslipidemia, so it can be considered a new model for obese type 2 diabetes.<sup>8-10</sup> However, the details of the hemodynamics in SDT fatty rats remain uncertain. In this study, we investigated the usefulness of the SDT fatty rat as a new PAD animal model. We examined certain aspects of the hemodynamics in the SDT fatty rat such as hindlimb blood flow, platelet aggregation, coagulation, and cardiac output, and compared the endothelial function of SDT fatty rats with that of normal Sprague–Dawley (SD) rats. Furthermore, we established a hindlimb ischemia model in SDT fatty rats and compared their responses to ischemia with those of SD rats.

## **Results**

### **Biological parameters**

Body weight and blood chemical parameters (glucose [Glu], triglyceride [TG], and total cholesterol [TC]) in the SDT fatty rats are presented in Table 1. As previously reported,<sup>8</sup> the plasma levels of Glu, TG, and TC in the SDT fatty rats at 5, 15, and 35 weeks of age were significantly higher than those in the SD rats (Table 1). The results confirmed that the SDT fatty rats used in this study developed metabolic disorders such as hyperglycemia, hyperlipidemia, and obesity.

### **Hemodynamics and endothelial function**

We first examined hindlimb blood flow in the SDT fatty rats and found that it was significantly lower than that in the SD rats at 5, 15, and 35 weeks of age (Fig. 1A, B). Because the SDT fatty rats showed metabolic disorder, they could produce excessive reactive oxidative species (ROS). The level of plasma nitrogen oxides (NOx), stable metabolites of NO, is often used as an oxidative stress marker.<sup>11</sup> To investigate the production of ROS in the SDT fatty rats, we measured the plasma NOx concentration and found that it was significantly higher in the SDT fatty rats than in the SD rats at 5, 15, and 35 weeks of age (Fig. 1C).

Hamilton and Watts reported that endothelial dysfunction causes impaired blood flow.<sup>12</sup> To evaluate endothelial function in the SDT fatty rats, we examined the expression of endothelial nitric oxide synthase (eNOS) phosphorylated at Ser1177 (p-eNOS [Ser1177])

in the aorta using western blot analysis. The ratio of p-eNOS (Ser1177) to total eNOS (T-eNOS) in the SDT fatty rats at 5 and 35 weeks of age ( $1.49 \pm 0.41$  and  $1.03 \pm 0.23$ , respectively) tended to be lower than that in the SD rats ( $1.90 \pm 0.55$  and  $1.61 \pm 0.72$ , respectively) (Fig. 2A, B). In addition, coagulation, platelet aggregation, and cardiac output were examined in the SDT fatty rats to elucidate the other mechanisms underlying lower hindlimb blood flow. The results showed that prothrombin time (PT), representing exogenous coagulation, and activated partial thromboplastin time (APTT), representing endogenous coagulation, were significantly shorter in the SDT fatty rats at 19 weeks of age (Fig. 2C, D). Maximum platelet aggregation induced by collagen tended to be higher in the SDT fatty rats ( $59.5\% \pm 17.1\%$ ) than in the SD rats ( $41.3\% \pm 13.7\%$ ) at 19 weeks of age (Fig. 2E). However, there was no difference in cardiac output between the two groups at 27 weeks of age (Fig. 2F).

### **Hindlimb ischemia model**

To investigate the blood flow response to ischemia in the hindlimb, we surgically induced hindlimb ischemia at 15 weeks of age. In this model, hindlimb blood flow decreased after surgery, then gradually recovered. The SDT fatty rats showed significantly lower blood flow before, immediately after and 7 and 14 days after ischemia induction (Fig. 3A, B). However, it was difficult to compare the reaction to ischemia between the two groups because the SDT fatty rats already had decreased blood flow before the induction of hindlimb ischemia (Fig. 1A, B). Therefore, we analyzed the

change in blood flow ( $\Delta$ blood flow) after hindlimb ischemia induction (Fig. 3C). The results showed that  $\Delta$ blood flow 7 days after ischemia induction was significantly lower in the SDT fatty rats than in the SD rats.

Angiogenesis causes the recovery of blood flow in the ischemic area. Thus, we examined angiogenesis immunohistopathologically in the SDT fatty rats after induction of hindlimb ischemia by immunostaining for the Von Willebrand Factor (VWF), an endothelial cell marker, and counting the number of VWF-positive vessels. This number for the SDT fatty rats was significantly less than that for the SD rats (Fig. 3D, E).



## **Discussion**

Several guidelines such as the American College of Cardiology/American Heart Association Guideline<sup>4</sup> and the Inter-Society Consensus for the Management of Peripheral Arterial Disease<sup>1</sup> recommend the use of supervised exercise, cilostazol, and revascularization as treatment for intermittent claudication. Although the most efficacious among the three treatments for intermittent claudication, supervised exercise is limited by the number of facilities that can provide it and by the physical and economic burdens it places on patients. Cilostazol is a phosphodiesterase 3 (PDE3) inhibitor and the only drug whose use for intermittent claudication is well supported by evidence.<sup>1,3</sup> However, cilostazol is contraindicated for patients with congestive heart failure. Furthermore, patient adherence to treatment with cilostazol is poor because of its side effects, including headache, dizziness, and palpitation. Revascularization, especially endovascular therapy, is very efficacious for treating intermittent claudication but has some disadvantages such as restenosis and placing physical and economic burdens on patients. Therefore, new therapies are needed to treat leg symptoms.

In nonclinical studies, the femoral artery ligation model is commonly used as a PAD model. In many cases, the femoral artery ligation model is created in nonmetabolic syndrome animals, such as C57BL/6J and BALB/c mice.<sup>13,14</sup> Although blood flow in ischemic limbs is decreased in this model, endothelial function and angiogenesis are not impaired because this model is based on normal animals. However, most PAD patients

show endothelial dysfunction<sup>5</sup> and poor angiogenesis<sup>15</sup> that are probably due to underlying diseases such as hypertension, diabetes, and dyslipidemia.<sup>1</sup> Therefore, in nonclinical studies, it is very important to evaluate the efficacy of drugs in a PAD model based on metabolic syndrome animals. Masuyama et al. reported that SDT fatty rats develop obesity, hyperglycemia, and dyslipidemia at a young age due to the transfer of the *fa* allele from the Zucker fatty rat to the genome of the nonobese SDT rat.<sup>8-10</sup> In this study, we found that hindlimb blood flow was significantly lower and the plasma NOx level was significantly higher in the SDT fatty rats compared with the SD rats. These results suggest that ROS production in the SDT fatty rats increased because of metabolic disorders such as hyperglycemia and hyperlipidemia. In addition, we found that the p-eNOS level tended to be lower in the SDT fatty rats at 5 and 35 weeks of age. Endothelial function in SDT fatty rats may be partly impaired by hyperglycemia, hyperlipidemia, and excess ROS production. Taken together, these findings suggest that the excess ROS and endothelial dysfunction in SDT fatty rats could be associated with the lower blood flow.

In addition to endothelial dysfunction, hypercoagulability affects peripheral blood flow, so we examined the association between lower blood flow, platelet aggregation, and platelet coagulation. We found that PT and APTT were significantly shorter and that the maximum platelet aggregation induced by collagen tended to be higher in the SDT fatty rats. Andersen et al. reported that hyperlipidemia is associated with increased coagulation.<sup>16</sup> In this study, the SDT fatty rats were hyperlipidemic, suggesting that

hyperlipidemia could cause the reduction of PT and APTT in SDT fatty rats, which might contribute to lower blood flow. Ohta et al. reported gender differences with respect to metabolic disorders in SDT fatty rats; female rats showed more severe insulin resistance and hyperlipidemia than male rats.<sup>17</sup> Therefore, female SDT fatty rats could show a marked reduction in PT and APTT, which could lead to severe blood flow reduction. It is very important to evaluate the gender differences with respect to lower blood flow to understand the pathology of SDT fatty rats.

We used the plasma NOx level as a measure of ROS production. Loffredo et al. used the plasma NOx level as a marker of NO production from eNOS (endothelial function).<sup>18</sup> Plasma NOx are stable NO metabolites and include NO<sup>2-</sup> and NO<sup>3-</sup>. Ignarro et al. showed that NO<sup>2-</sup> was produced by oxidation of NO, the same as the production of NO<sup>2-</sup> in air, while NO<sup>3-</sup> was produced by oxidation in the presence of ROS.<sup>19</sup> Therefore, the plasma NOx concentration might have a different meaning depending on pathology. Kobayashi et al. showed that STZ mice, a type 1 diabetes model, had elevated plasma NO<sup>3-</sup> and impaired endothelial function.<sup>20,21</sup> Therefore, we hypothesize that the increased plasma NOx in our SDT fatty rats might have been caused by an elevated plasma NO<sup>3-</sup> level. Measuring the plasma NO<sup>2-</sup> and NO<sup>3-</sup> levels in a future study will help elucidate the pathology of SDT fatty rats in greater detail.

We previously showed that sensory nerve conduction velocity (SNCV) in SDT fatty rats was significantly lower than that in SD rats.<sup>22</sup> Stevens et al. mentioned that metabolic

disorders such as hyperglycemia might induce endothelial dysfunction, which could lead to decreased nerve blood flow.<sup>23</sup> Therefore, we suggest that the decreased blood flow in SDT fatty rats might be associated with impaired SNCV.

We also evaluated hindlimb blood flow after surgically induced hindlimb ischemia in the SDT fatty rats. Blood flow in the hindlimb ischemia model is expressed as the ratio of ischemic to nonischemic hindlimb blood flow by many researchers. Blood flow in the SDT fatty rats was lower than that in the SD rats, not only in the ischemic limb but also in the nonischemic limb. Therefore, it is difficult to compare the ischemic/nonischemic ratio of the SDT fatty rats with that of the SD rats. However, we found that 7 days after ischemia induction, the SDT fatty rats had significantly decreased blood flow. Furthermore, in this study, the number of VWF-positive vessels in gastrocnemius muscles decreased in the SDT fatty rats, suggesting that angiogenesis had decreased. Schiekofer et al. reported that blood flow recovery in diabetic *db/db* mice significantly deteriorated than that in C57BL/6J mice.<sup>6</sup> They also showed that adductor muscles in *db/db* mice after ligation had decreased angiogenesis and mRNA expression of VEGF-A, a well-known angiogenesis factor, compared with those in C57BL/6J mice.<sup>6</sup> Therefore, the expression of VEGF-A mRNA in SDT fatty rats might be reduced.

Although the SDT fatty rats in our study showed impaired angiogenesis, hindlimb blood flow recovered after surgically induced hindlimb ischemia. Thus, angiogenesis in the SDT fatty rats might not have been completely disturbed. However, arteriogenesis also

contributes to the recovery of blood flow in ischemic limbs<sup>24</sup> and could be involved in the recovery of blood flow after induction of hindlimb ischemia.

Bhatt et al. found that diabetes and hypercholesterolemia were complications in 44.2% and 66.7% of PAD patients, respectively.<sup>25</sup> In another study, flow-mediated dilation (FMD), an endothelial function marker, was lower in PAD patients than in healthy volunteers,<sup>5</sup> suggesting that endothelial function in PAD patients is impaired.<sup>5</sup> Furthermore, Kikuchi et al. reported that the increase in the level of VEGF-A165b, an antiangiogenic VEGF-A splice isoform, may be involved in the impairment of angiogenesis in PAD patients.<sup>26</sup> Also, hyperglycemia and endothelial dysfunction develop in SDT fatty rats and, as in PAD patients, cause impaired angiogenesis after ischemia. Therefore, SDT fatty rats might be similar to PAD patients in terms of basic phenotype and response to ischemia. We will examine the VEGF-A165b level in SDT fatty rats in a future study.

In conclusion, we found that SDT fatty rats had lower-than-normal hindlimb blood flow under nonischemic conditions. We showed that excess ROS production, the activation of coagulation and platelet aggregation, and endothelial dysfunction might have contributed to the lower blood flow. Furthermore, we showed that the recovery of hindlimb blood flow after induction of hindlimb ischemia in SDT fatty rats was impaired by poor angiogenesis. Taken together, these results indicate that SDT fatty rats may be useful as a new model for PAD with metabolic syndrome.

## **MATERIALS AND METHODS**

### **Animals**

All experiments were conducted at the Japan Tobacco Central Pharmaceutical Research Institute and were in compliance with the Guidelines for Animal Experimentation. Male 4-week-old SDT fatty rats and age-matched male SD rats used as normal control rats were purchased from CLEA Japan, Inc. (Tokyo, Japan). The rats were maintained in suspended bracket cages and fed a standard laboratory diet (CRF-1, Oriental Yeast Co., Ltd., Tokyo, Japan) and water ad libitum under temperature-, humidity-, and lighting-controlled conditions.

### **Biological parameters**

Body weight and nonfasting plasma biochemical parameters, such as Glu, TG, and TC levels, were measured at 5, 15, and 35 weeks of age. Blood samples were collected from the tail veins of the rats. The plasma Glu, TG, and TC levels were measured using commercial kits (Roche Diagnostics K.K., Tokyo, Japan) and an automatic analyzer (Hitachi, Ltd., Tokyo, Japan).

### **Plasma NOx**

To measure the plasma NOx level, proteins were removed from plasma by centrifugation at 16,000 *g* and 4°C for 20 min using an Amicon<sup>®</sup> Ultra-0.5 Centrifugal Filter Device (Millipore Corporation, Billerica, MA, USA) and then the flow-through was collected. NOx in the flow-through was measured using a QuantiChrom<sup>™</sup> Nitric Oxide Assay Kit

(BioAssay Systems, Hayward, CA, USA).

### **Hindlimb ischemia model**

Hindlimb ischemia was induced in 15-week-old SDT fatty rats and SD rats (as controls). After anesthetizing the rats with 2% isoflurane, hindlimb ischemia was induced in the left leg by ligation of the proximal femoral artery and the distal saphenous artery. The two ligation sites and all branches between them were excised. Skin incision without right femoral artery ligation was performed as a sham operation.

### **Laser Doppler perfusion imaging**

Hindlimb blood flow was measured with a laser Doppler perfusion imager (Moor Instruments Limited, Axminster, UK). Before measuring hindlimb blood flow, the rats were anesthetized with 2% isoflurane and placed on a warming plate to maintain constant body temperature. During laser Doppler perfusion imaging (LDPI), the rats were anesthetized with 1.5% isoflurane. Hindlimb blood flow was measured at 5, 15, and 35 weeks of age in the nonischemic rats, and before the ischemia-inducing operation, immediately after arterial excision, and 7 and 14 days after induction of hindlimb ischemia in the ischemic rats.

### **Western blot analysis**

Aortas were homogenized in 0.3 mL of radioimmunoprecipitation assay (RIPA) buffer (Cell Signaling Technology, Inc., Danvers, MA, USA) containing 1 mM phenylmethylsulfonyl fluoride (PMSF) and cOmplete™ ULTRA Tablets, Mini,

EASYpack protease inhibitor cocktail (Hoffmann-La Roche Ltd., Basel, Switzerland). The homogenates were then centrifuged at 16,000 *g* and 4°C for 10 min and the supernatants underwent western blot analysis to quantify the protein levels of eNOS and p-eNOS (Ser1177). The tissue lysate was solubilized in NuPAGE™ LDS Sample Buffer (Thermo Fisher Scientific K.K., Tokyo, Japan) containing NuPAGE™ Sample Reducing Agent (Thermo Fisher Scientific K.K.). Samples (20-40 µg/lane) were resolved by electrophoresis on 4%-12% SDS-PAGE gels (Thermo Fisher Scientific K.K.) and then transferred onto polyvinylidene difluoride (PVDF) membranes. The PVDF membranes were blocked with Blocking One (Nacalai Tesque, Inc., Kyoto, Japan) and then incubated with either anti-eNOS (140 kDa; 1:1000, Cell Signaling Technology, Inc.), antiphosphorylated eNOS (Ser1177) (140 kDa; 1:1000, Cell Signaling Technology, Inc.), or antibody to β-actin (42 kDa; 1:1000, Cell Signaling Technology, Inc.) (the housekeeping protein used to normalize the data) in 10% Blocking One-TBS with Tween 20 solution. Horseradish peroxidase (HRP)-conjugated anti-rabbit antibody (GE Healthcare Life Sciences, Chicago, IL, USA) was used at 1:5000 dilution in 10% Blocking One-TBS with Tween 20 solution. The optical densities of the bands on the membrane were quantified using an Amersham Imager 680 (GE Healthcare Life Sciences).

### **Immunostaining**

The vessels were flushed with phosphate-buffered saline (PBS) and heparin (250 U/kg)



14 days after hindlimb ischemia surgery. Perfusion-fixation was performed using 4% paraformaldehyde phosphate buffer solution (Nacalai Tesque, Inc.) and the gastrocnemius muscle was harvested. The tissue was then embedded in paraffin, cut into 5- $\mu$ m sections, and stained with VWF antibody (1:400, Abcam plc, Cambridge, UK). Capillary density was quantified by measuring the number of VWF-positive vessels on an image of the total gastrocnemius muscle area obtained with a BIOREVO BZ-9000 fluorescence microscope (KEYENCE Corp., Osaka, Japan).

#### **Platelet aggregation activity assay**

Blood samples were collected from the SDT fatty rats and the SD rats at 19 weeks of age. Sodium citrate (3.8% w/v) solution was mixed with the blood in a blood:sodium citrate solution ratio of 9:1. Each blood sample was centrifuged at 170 g and room temperature for 10 min, and the supernatant was collected as platelet-rich plasma (PRP). The remaining blood sample was centrifuged at 1000 g and room temperature for 15 min to obtain platelet-poor plasma (PPP). The number of platelets was measured using a Sysmex KX-21NV Hematology Analyzer (Sysmex Corporation, Kobe, Japan), and the PRP was diluted in PPP so that the number of platelets was  $3.0 \times 10^4/\mu\text{L}$ . Platelet aggregation activity was determined using a HAMA TRACER 712 (MC Medical, Inc., Tokyo, Japan). Exactly 0.29 mL of the diluted PRP was transferred to a siliconized cuvette that was then placed in a PRP chamber. The final volume in the cuvette was 0.30 mL after the addition 10  $\mu\text{L}$  of collagen (7  $\mu\text{M}$ ). For reference, a cuvette containing

0.30 mL of PPP was placed in a PPP chamber. PRP was preincubated for 2 min, then incubated for 7 min after the addition of 10  $\mu$ L of collagen, and finally observed to detect collagen-induced platelet aggregation.

### **Coagulation assay**

Blood samples were collected as described in the preceding subsection. Each blood sample was centrifuged at 1000 *g* and room temperature for 15 min to separate the plasma. PT and APTT were measured using an ACL Elite PRO automatic coagulometer (IL Japan, Tokyo, Japan).

### **Echocardiographic parameters**

Echocardiography was performed in 27-week-old rats under anesthesia as follows: The heart rate was maintained at approximately 320 beats per minute with the use of 2% isoflurane. The left ventricular anterior wall, LV end-diastolic dimension, LV end-systolic dimension, and LV posterior wall were measured on the short-axis view using the M-mode method, and the LV ejection fraction was automatically calculated from the LV end-diastolic volume and LV end-systolic volume.

### **Statistical analysis**

All data are expressed as the mean  $\pm$  standard deviation. A two-group comparison was performed using the F test, followed by the Student *t* test or the Aspin-Welch *t* test. Differences were considered significant at  $p < 0.05$ .

## **ACKNOWLEDGMENTS**

We thank the editing service of John Wiley & Sons (<http://wileyeditingservices.com>) for the English language editing of this paper. We also thank Dr. Tatsuya Maekawa and Dr. Yasufumi Toriniwa for their assistance in this study.

## **CONFLICT OF INTERESTS**

The authors have no conflicts of interest directly relevant to the content of this article.

## References

1. Norgren L, Hiatt WR, Dormandy JA, et al. Inter-Society Consensus for the Management of Peripheral Arterial Disease (TASC II). *Journal of Vascular Surgery*. 2007;45 Suppl S:S5-67.
2. Ohman EM, Bhatt DL, Steg PG, et al. The REduction of Atherothrombosis for Continued Health (REACH) Registry: an international, prospective, observational investigation in subjects at risk for atherothrombotic events-study design. *American Heart Journal*. 2006;151(4):786 e781-710.
3. Stewart KJ, Hiatt WR, Regensteiner JG, et al. Exercise training for claudication. *New England Journal of Medicine*. 2002;347(24):1941-1951.
4. Gerhard-Herman MD, Gornik HL, Barrett C, et al. 2016 AHA/ACC Guideline on the Management of Patients with Lower Extremity Peripheral Artery Disease: Executive Summary: A Report of the American College of Cardiology/American Heart Association Task Force on Clinical Practice Guidelines. *Journal of the American College of Cardiology*. 2017;69(11):1465-1508.
5. Sanada H, Higashi Y, Goto C, et al. Vascular function in patients with lower extremity peripheral arterial disease: a comparison of functions in upper and lower extremities. *Atherosclerosis*. 2005;178(1):179-185.
6. Schiekofer S, Galasso G, Sato K, et al. Impaired revascularization in a mouse model of type 2 diabetes is associated with dysregulation of a complex angiogenic-

- regulatory network. *Arteriosclerosis, Thrombosis, and Vascular Biology*. 2005;25(8):1603-1609.
7. Yan J, Tie G, Park B, et al. Recovery from hind limb ischemia is less effective in type 2 than in type 1 diabetic mice: roles of endothelial nitric oxide synthase and endothelial progenitor cells. *Journal of Vascular Surgery*. 2009;50(6):1412-1422.
  8. Masuyama T, Katsuda Y, Shinohara M. A novel model of obesity-related diabetes: introgression of the *Lepr<sup>fa</sup>* allele of the Zucker fatty rat into nonobese Spontaneously Diabetic Torii (SDT) rats. *Experimental Animals*. 2005;54(1):13-20.
  9. Katsuda Y, Ohta T, Miyajima K, et al. Diabetic complications in obese type 2 diabetic rat models. *Experimental Animals*. 2014;63(2):121-132.
  10. Toriniwa Y, Saito T, Miyajima K, et al. Investigation of pharmacological responses to anti-diabetic drugs in female Spontaneously Diabetic Torii (SDT) fatty rats, a new nonalcoholic steatohepatitis (NASH) model. *Journal of Veterinary Medical Science*. 2018;80(6):878-885.
  11. Giriwono PE, Shirakawa H, Hokazono H, et al. Fermented barley extract supplementation maintained antioxidative defense suppressing lipopolysaccharide-induced inflammatory liver injury in rats. *Bioscience, Biotechnology, and Biochemistry*. 2011;75(10):1971-1976.
  12. Hamilton SJ, Watts GF. Endothelial dysfunction in diabetes: pathogenesis, significance, and treatment. *Review of Diabetic Studies: RDS*. 2013;10(2-3):133-156.

13. Masaki I, Yonemitsu Y, Yamashita A, et al. Angiogenic gene therapy for experimental critical limb ischemia: acceleration of limb loss by overexpression of vascular endothelial growth factor 165 but not of fibroblast growth factor-2. *Circulation Research*. 2002;90(9):966-973.
14. Yu J, deMuinck ED, Zhuang Z, et al. Endothelial nitric oxide synthase is critical for ischemic remodeling, mural cell recruitment, and blood flow reserve. *Proceedings of the National Academy of Sciences of the United States of America*. 2005;102(31):10999-11004.
15. Hamburg NM, Creager MA. Pathophysiology of Intermittent Claudication in Peripheral Artery Disease. *Circulation Journal: Official Journal of the Japanese Circulation Society*. 2017;81(3):281-289.
16. Andersen P. Hypercoagulability and reduced fibrinolysis in hyperlipidemia: relationship to the metabolic cardiovascular syndrome. *Journal of Cardiovascular Pharmacology*. 1992;20 Suppl 8:S29-31.
17. Ohta T, Katsuda Y, Miyajima K, et al. Gender differences in metabolic disorders and related diseases in Spontaneously Diabetic Torii-Lepr(fa) rats. *Journal of Diabetes Research*. 2014;2014:841957.
18. Loffredo L, Marcoccia A, Pignatelli P, et al. Oxidative-stress-mediated arterial dysfunction in patients with peripheral arterial disease. *European Heart Journal*. 2007;28(5):608-612.

19. Ignarro LJ, Fukuto JM, Griscavage JM, et al. Oxidation of nitric oxide in aqueous solution to nitrite but not nitrate: comparison with enzymatically formed nitric oxide from L-arginine. *Proceedings of the National Academy of Sciences of the United States of America*. 1993;90(17):8103-8107.
20. Kobayashi T. [Possible involvement of insulin and oxidative stress in vascular dysfunction of diabetic mellitus]. *Yakugaku Zasshi: Journal of the Pharmaceutical Society of Japan*. 2008;128(7):1013-1021.
21. Jelic-Knezovic N, Galijasevic S, Lovric M, et al. Levels of Nitric Oxide Metabolites and Myeloperoxidase in Subjects with Type 2 Diabetes Mellitus on Metformin Therapy. *Experimental and Clinical Endocrinology & Diabetes: Official Journal, German Society of Endocrinology [and] German Diabetes Association*. 2019;127(1):56-61.
22. Murai Y, Ohta T, Tadaki H, et al. Assessment of Pharmacological Responses to an Anti-diabetic Drug in a New Obese Type 2 Diabetic Rat Model. *Medical Archives*. 2017;71(6):380-384.
23. Stevens MJ. Nitric oxide as a potential bridge between the metabolic and vascular hypotheses of diabetic neuropathy. *Diabetic Medicine: Journal of the British Diabetic Association*. 1995;12(4):292-295.
24. Carmeliet P. Mechanisms of angiogenesis and arteriogenesis. *Nature Medicine*. 2000;6(4):389-395.

25. Bhatt DL, Steg PG, Ohman EM, et al. International prevalence, recognition, and treatment of cardiovascular risk factors in outpatients with atherothrombosis. *JAMA*. 2006;295(2):180-189.
26. Kikuchi R, Nakamura K, MacLauchlan S, et al. An antiangiogenic isoform of VEGF-A contributes to impaired vascularization in peripheral artery disease. *Nature Medicine*. 2014;20(12):1464-1471.



## Tables

Table 1. Biological parameters in SDT fatty rats.

		5 wk			15 wk			35 wk		
BW	SD	118.6	±	2.8	562.1	±	38.4	783.5	±	68.4
(g)	SDT fatty	197.6	±	5.4**	531.1	±	20.6	500.9	±	25.0**
Glu	SD	144.5	±	4.0	127.5	±	7.0	160.5	±	13.1
(mg/dL)	SDT fatty	291.0	±	92.7*	797.0	±	43.8**	842.5	±	206.9**
TG	SD	228.0	±	147.6	238.3	±	66.9	262.8	±	82.0
(mg/dL)	SDT fatty	206.6	±	29.9	429.4	±	99.9**	446.3	±	103.5**
TC	SD	83.9	±	11.6	75.7	±	10.0	103.8	±	13.0
(mg/dL)	SDT fatty	121.9	±	4.9**	152.2	±	12.5**	167.4	±	32.4**

BW = body weight, Glu = glucose, TG = triglyceride, TC = total cholesterol

Data are presented as mean ± standard deviation ( $n = 6$ ).

\* $p < 0.05$ , \*\* $p < 0.01$ : significantly different from the SD rats.

## Figure legends

Figure 1: Hindlimb blood flow and plasma NO<sub>x</sub> in SDT fatty rats and SD rats at 5, 15, 35 weeks of age. (A) Representative laser Doppler perfusion imaging. Blue indicates low blood flow and red indicates high blood flow. (B) Quantitative blood flow analysis using laser Doppler perfusion imaging data. (C) Plasma NO<sub>x</sub>. Data are presented as mean ± standard deviation ( $n = 6$ ).  $**p < 0.01$  means significantly different from the SD rats.

Figure 2: Endothelial function, platelet aggregation activity, coagulation activity, and cardiac output in SDT fatty rats and SD rats. (A) Western blot analysis of phosphorylated eNOS (p-eNOS) and total eNOS (T-eNOS) in aortas at 35 weeks of age. (B) Quantitative Western blot analysis at 5 and 35 weeks of age. eNOS level is expressed as the p-eNOS/T-eNOS ratio. (C-E) PT, APTT, and maximum platelet aggregation activity induced by 7 μM of collagen at 19 weeks of age. (F) Left ventricular ejection fraction (LVEF) at 27 weeks of age. Data are presented as mean ± standard deviation ( $n = 6$ ).  $*p < 0.05$  means significantly different from the SD rats,  $**p < 0.01$  means significantly different from the SD rats.

Figure 3: Hindlimb blood flow and angiogenesis in SDT fatty rats and SD rats after inducing hindlimb ischemia at 15 weeks of age. (A) Representative laser Doppler perfusion imaging before surgery, immediately after arterial excision, and 7 and 14 days after induction of hindlimb ischemia. Blue indicates low blood flow and

red indicates high blood flow. (B) Quantitative blood flow analysis using laser Doppler perfusion imaging data. (C) Change in blood flow ( $\Delta$ blood flow) after induction of hindlimb ischemia. (D) Gastrocnemius muscles 14 days after induction of hindlimb ischemia, immunostained for VWF. Arrowheads indicate VWF positive vessels. (E) Quantitative analysis of the VWF-positive vessels per total gastrocnemius muscle area. Data are presented as mean  $\pm$  standard deviation ( $n = 4-5$ ).  $*p < 0.05$  means significantly different from the SD rats,  $**p < 0.01$  means significantly different from the SD rats.

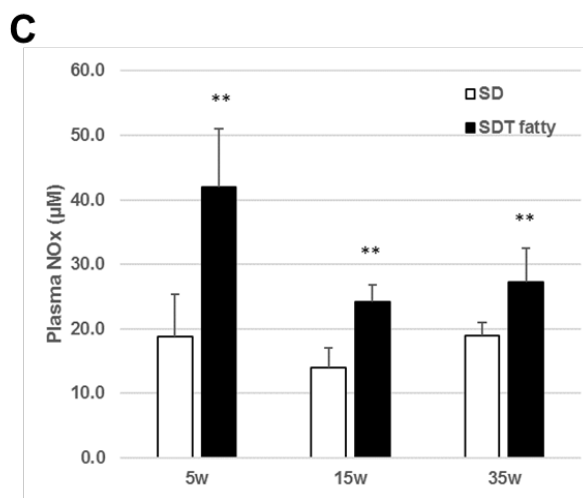
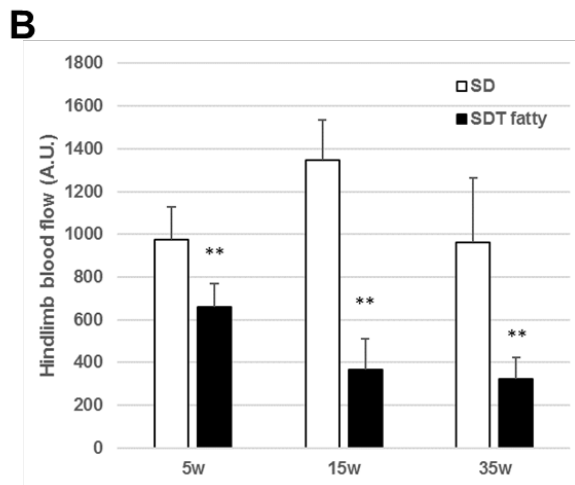
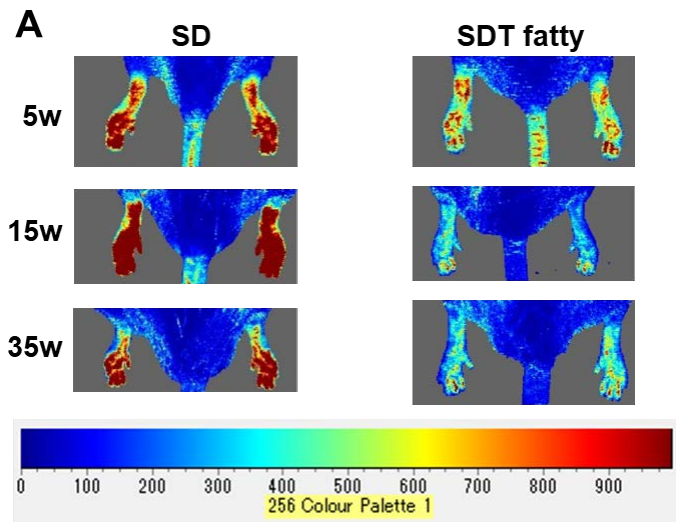


Figure 1

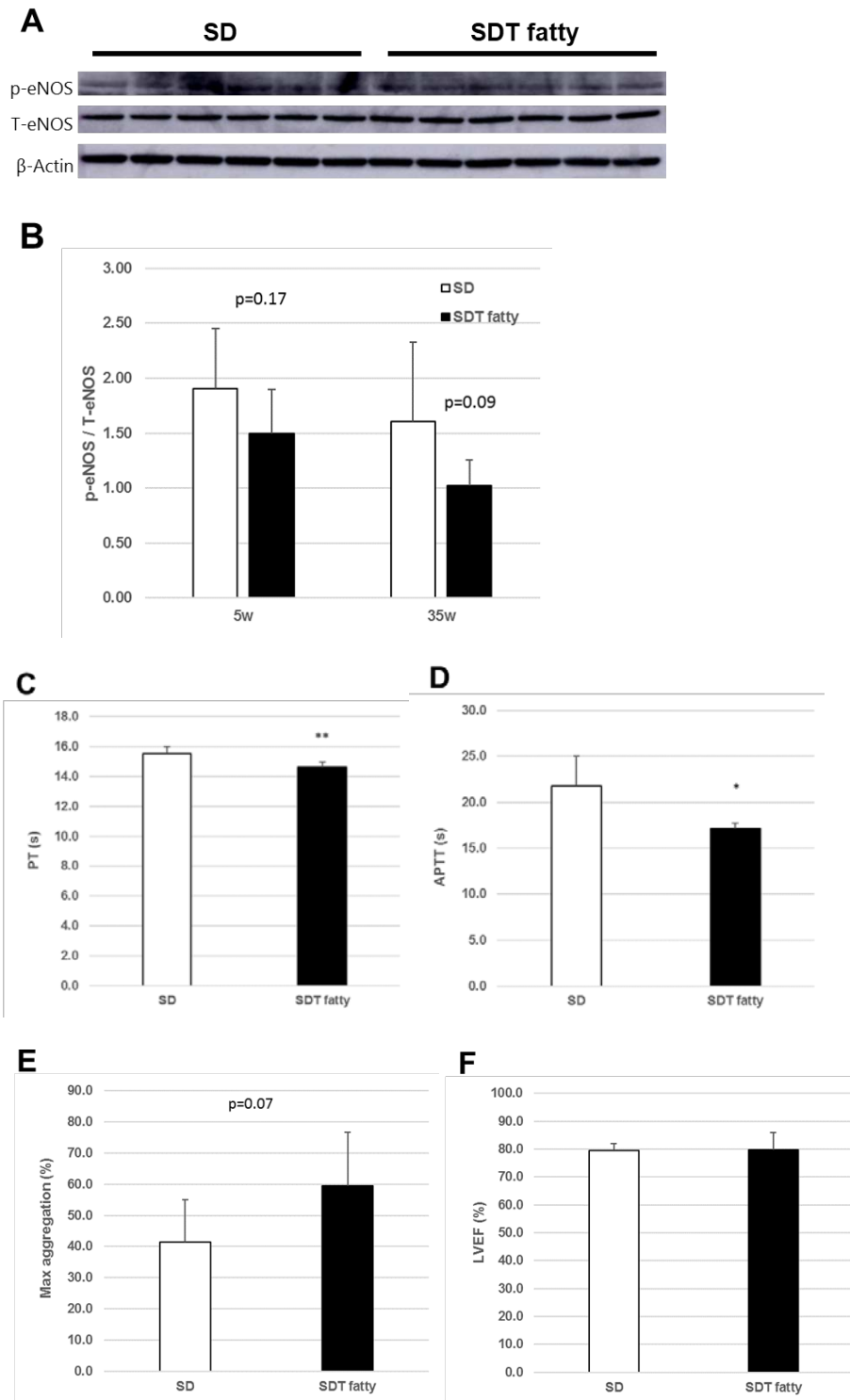


Figure 2

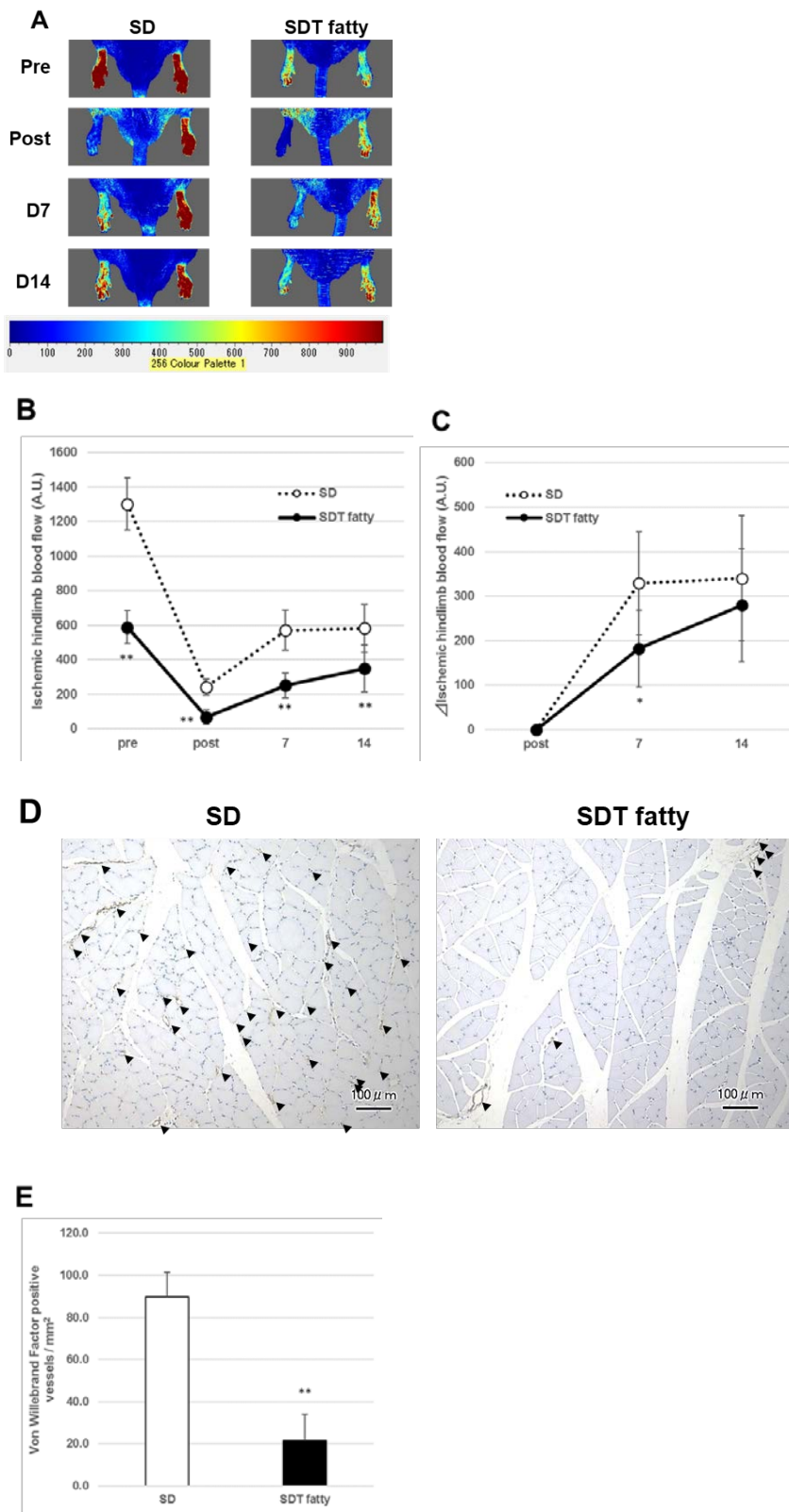


Figure 3